Analysis of Flip Ambiguities for Robust Sensor Network Localization

Anushiya A. Kannan, *Member, IEEE*, Barış Fidan, *Member, IEEE*, and Guoqiang Mao, *Senior Member, IEEE*

***Abstract*—Erroneous local geometric realizations in some parts of a network due to the sensitivity to certain distance-measurement errors with respect to some neighboring sensor locations is a major problem in wireless sensor-network localization, which may, in turn, affect the reliability of the localization of the whole or a major portion of the sensor network. This phenomenon is well described using the notion of "flip ambiguity" in rigid graph theory. In this paper, we present a formal geometric analysis of flip-ambiguity problems in planar sensor networks via quantification of the likelihood of flip ambiguities in arbitrary sensor neighborhood geometries. Based on this analysis, we establish a robustness criterion to detect flip ambiguities in such neighborhood geometries. In addition to the analysis, the established robustness criterion is embedded in localization algorithms to enhance the reliability of the produced location estimates by eliminating neighborhoods with flip ambiguities from being included in the localization process.**

***Index Terms*—Flip ambiguities in WSN localization, robust WSN localization.**

I. Introduction

RECENT advances in integrated circuit design, embedded systems, and wireless communication technology have enabled smart tiny sensors to be deployed in large numbers. Most of these sensor nodes will be deployed at positions that may not be predetermined due to constraints on the implementation environment and/or the cost of deployment at known locations. The information gathered by such sensor nodes, in general, will be useless without determining the locations of these nodes. This makes self-localization capabilities a highly desirable characteristic of sensor networks [1]–[4]. Sensor network-localization algorithms use intersensor measurements, which can be in the form of distance measurements, bearing measurements, time-difference-of-arrival measurements, etc., and the *a priori* known locations of some specific sensors, which can be usually obtained via the Global Positioning System or by deploying sensors at known locations, to estimate the locations of all sensors in the network. This paper focuses on distance-measurement-based localization algorithms.

Based on the approach of processing the distance measurements, distance-based localization algorithms can be categorized into two main classes [5]: centralized algorithms and distributed algorithms. Centralized algorithms [5]–[8] use a single central processor to collect all distance measurements between neighboring nodes and produce a map of the entire sensor network, while distributed algorithms [5], [9]–[11] rely on the self-localization of each sensor node in a sensor network using the distance measurements they collect from one-hop and multihop neighbors and the *a priori* known or estimated locations of these neighbors.

A fundamental problem in distance-based sensor network localization is whether a given sensor network is uniquely localizable or not, i.e., whether the sensor network geometry corresponding to known locations of some specific sensors and a given set of intersensor distance measurements is unique or not. A particular framework that is useful for analyzing this problem is *rigid graph theory* [12]–[15]. In this framework, the sensor network to be localized is modeled by a graph called the *underlying graph* of the sensor network, where the vertices of the graph represent sensor nodes, and all the vertex pairs corresponding to the sensor node pairs with known distance measurements are connected with edges.

If the actual geometries of some parts of the sensor network are sensitive to distance measurement errors, it may cause erroneous local geometric realizations in those parts of the network.[1] This is a major problem affecting the unique realizability of the distance-based localization [4], [6], [7]. One such phenomenon is *flip ambiguity*, which can prevent unique localization of the sensor network [14]–[17] (in the sense that it differs from other such representations at most by translation, rotation, or reflection).

In flip ambiguities, a sensor node (or sensor nodes) with a set of neighbors that are almost collinear may lead to the possibility of the neighbors forming a mirror through which the sensor node (or the sensor nodes) can be reflected, thereby causing a large localization error. Moreover, when the localization algorithm proceeds, it is likely to continue degrading the location estimates in the subsequent iterations that use the location estimate of the flipped sensor nodes. This impact can propagate in an avalanche fashion for several iterations, affecting, in turn, the location estimates of either the entire network or a large portion

Manuscript received June 22, 2009; revised October 12, 2009. First published February 8, 2010; current version published May 14, 2010. This work was supported by the National Information and Communications Technologies (ICT) Australia, which is funded by the Australian Government as represented by the Department of Broadband, Communications, and the Digital Economy and the Australian Research Council through the ICT Centre of Excellence Program. The review of this paper was coordinated by Dr. P. Lin.

A. A. Kannan is with the University of Sydney, Sydney, NSW 2006, Australia, and also with the Biomedical Systems Laboratory, University of New South Wales, Sydney, NSW 2052, Australia (e-mail: Anushiya.Kannan@nicta.com.au).

B. Fidan is with the Department of Mechanical and Mechatronics Engineering, University of Waterloo, Waterloo, ON N2L 3G1, Canada (e-mail: fidan@uwaterloo.ca).

G. Mao is with the School of Electrical and Information Engineering, University of Sydney, Sydney, NSW 2006, Australia (e-mail: Guoqiang.Mao@nicta.com.au).

Color versions of one or more of the figures in this paper are available online at http://ieeexplore.ieee.org.

Digital Object Identifier 10.1109/TVT.2010.2040850

[1] Although similar problems may also exist in localization tasks based on other types of measurement techniques, we focus only on distance-based localization.

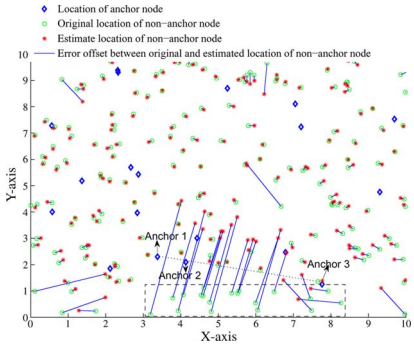

Fig. 1. Avalanche error propagation of flip ambiguity seen in a centralized localization algorithm presented in [8]. The anchor nodes marked as 1, 2, and 3 are placed almost collinearly and cause a large number of flipped realizations in the location estimates of sensor nodes shown within the rectangle.

of it. This behavior of avalanche error propagation can be noticed in many localization algorithms in the literature. Fig. 1 shows one such avalanche error propagation in a centralized algorithm [8]. In the bottom part of Fig. 1, the three anchors noted as anchors 1, 2, and 3 are placed almost collinearly. This causes a large number of sensor nodes (shown within the rectangle in Fig. 1), which may not necessarily be the one-hop neighbors of these three anchors, to be flipped to incorrect positions, thereby resulting in large location-estimation errors in the system. A detailed description of flip ambiguities and the resulting avalanche error-propagation effects are given in Sections III and IV.

An empirical study on the frequency of flip-ambiguity occurrences is presented in [18]. This study shows that with an increasing number of neighbors of a location-unknown sensor node, the frequency of flipped realizations reduces (but never gets to zero). Moreover, at the initial stages of any localization algorithm, many neighbors will not know their locations, and locations are estimated with a smaller number of neighbors, causing more frequent occurrences of flip ambiguities. When the localization algorithm proceeds, it is likely for the number of neighbors to grow, reducing the frequency of flip ambiguities. However, if the set of neighbors contains any flipped realized sensor node, it can cause the flip-ambiguity effect to propagate in the rest of the localization process. This may, in turn, affect the localization of the whole or a major part of the sensor network, as explained in Section IV.

Flip ambiguities do not necessarily occur in every sensor network, but when they occur, they can significantly degrade the localization of the whole network (as shown in Fig. 1). It is therefore important to identify possible flip ambiguities in the location estimates and take proper action to prevent them from being used in the localization process.

This paper proposes a robustness criterion to identify the likelihood of flip ambiguities in arbitrary sensor neighborhoods, which is applied on all neighborhoods to identify the sensor nodes contributing to flip ambiguity and eliminate them from the neighborhoods used in the localization process. Thus, with the help of the robustness criterion, the localization algorithm selects the robust neighborhoods containing only the sensor nodes that do not contribute to flip ambiguities. Even though the selection of robust neighborhoods will mitigate flip ambiguity in both centralized and distributed localization algorithms, this paper focuses only on the performance improvement in distributed localization.

The rest of this paper is organized as follows. Section II summarizes the related work in the literature. Section III presents a brief overview of a theoretical framework of unique sensor network localization and the associated ambiguities. Section IV explains the effects of flip ambiguities in localization algorithms using simple examples and how error propagates following the occurrence of a flipped realization. Section V analyzes the effects of neighborhood geometries on flip ambiguities and formulates the problem of identifying flip ambiguities in sensor neighborhoods. Section VI proposes a robustness criterion to identify possible neighborhoods with a high probability of having flip ambiguities. Section VII presents a numerical analysis of the effectiveness of the derived robustness criterion in the removal of flipped realizations. Section VIII explains a localization algorithm using our robustness criterion and presents the simulation results demonstrating the performance enhancement. Section IX presents a more application-oriented version of the localization algorithm presented in Section VIII, which increases the number of localized nodes with negligible degradation in estimation errors. This paper is concluded in Section X.

II. Related Work

In the literature, the flip-ambiguity problem has been approached from different perspectives to eliminate their effect on the location estimation of the sensor nodes. The main aim of these methods is to estimate the locations of the sensor nodes with minimum error.

The notions of Voronoi diagrams and Delaunay graphs are used in [19] and [20] to glue the Delaunay triangles in an incremental fashion to achieve unique localization of boundary or landmark sensors. These sensors are then used as anchors to localize the rest of the network. Such a method requires the boundary/landmark sensors to be sufficiently dense to maintain the global rigidity of the Delaunay graph. The underlying graph structure of the sensor network is explored in [14], [17], and [19] to obtain unique localization. The algorithms in [14] and [17] maintained global rigidity, which is a sufficient condition for unique localization, by having a denser network. The concept of global rigidity is defined later in Section III-A.

Designing an efficient distributed algorithm for global rigidity, however, is nontrivial, as neither connectivity nor rigidity can be tested locally by nature [21]. In practice, trilateration [15], [22]–[26] is widely used to localize the unknown sensor nodes, as it is fully distributed and easily implementable. The study in [21] pointed out that wheel graphs are globally rigid and that trilateration is a special case of wheel graphs.

Global rigidity is, however, only a sufficient condition for the unique localization of a sensor network. *A priori* information may compensate the need for global rigidity in some graph structure [4]. Moreover, the graph realization theory does not account for measurement errors affecting intersensor measurements in real applications [25]. For sparse networks with noisy measurements, the algorithms in [27] and [28] recorded all possible location estimates of each sensor and eliminate the incompatible location estimates whenever possible, which, in the worst case, can result in an exponential space requirement.

Another approach for mitigating flip ambiguity in noisy environments is to identify possible flip ambiguities in location estimates and take the necessary action to eliminate such

flip ambiguities from the localization process [15], [25], [26]. The studies in [15] and [25] use the trilateration-based sensor quadruple, which is a four-sensor neighborhood structure, to derive robust criteria to identify possible flip ambiguity in location estimates of sensor nodes. Only the sensor quadruples that are identified as not susceptible to flip ambiguities by the robustness criterion are tagged as robust neighborhoods and are used in the localization process. The study in [26] provided a formal geometric analysis of the flip-ambiguity problem using similar notions as those in [15] and [25]. It developed a generic formal method for quantifying the likelihood of flip ambiguities for arbitrary sensor neighborhood geometries.

The analyses in [15], [25], and [26] have been conducted under the assumption of unknown sensor nodes having access to intersensor distance measurements from all three of its neighbors, where only one distance measurement is considered to be in error, while the other two are considered accurate.

Our paper also considers completely connected sensor quadruples in a planar sensor network and establishes a robustness criterion to identify possible flip ambiguities. In contrast to [15], [25], and [26], which consider unique localizability with only one erroneous distance measurement while assuming all the other distance measurements are accurate, our paper accommodates the errors in one or more intersensor distance measurements. Furthermore, unlike the work in [15], [25], and [26], which restricted the localization to trilateration using the sensor quadruples, our work uses a novel way to select all neighbors that do not contribute to flip ambiguities (which is explained in Section VIII) and to use them in the localization algorithm with a multilateration scheme.

III. Graph-Theoretical Framework for Sensor Network Localization

A. Modeling for Unique Sensor Network Localization

In a graph-theoretical framework, a sensor network can be represented by a graph $G = (V, E)$ with a vertex set V and an edge set E, where each vertex $X \in V$ is uniquely associated with a sensor node s_X in the network, and each edge $(X, Y) \in E$ uniquely corresponds to a sensor node pair (s_X, s_Y) for which the intersensor distance is known [12]–[17], [29]. The graph $G(V, E)$ is called the underlying graph of the network.

The planar location information about the sensor nodes corresponds to a 2-D *representation* of the representative graph, which is a mapping $p : V \to \mathcal{R}^2$, assigning a location in $\mathcal{R}^2$ to each vertex in V. Given a graph $G = (V, E)$ and a representation of it, the pair (G, p) is called a *framework*.

A particular graph property associated with the unique realizability of sensor networks is *global rigidity* [4], [12], [13], [29]. A framework (G, p) is globally rigid if every framework (G, p_1) satisfying $\|p(X) - p(Y)\| = \|p_1(X) - p_1(Y)\|$ for any vertex pair $X, Y \in V$, which are connected by an edge in E, also satisfies the same equality for any other vertex pairs that are not connected by an edge. A relaxed form of global rigidity is *rigidity*: a framework (G, p) is rigid if there exists a sufficiently small positive constant ϵ such that every framework (G, p_1) satisfying 1) $\|p(X) - p_1(X)\| < \epsilon$ for all $X \in V$ and 2) $\|p(X) - p(Y)\| = \|p_1(X) - p_1(Y)\|$ for any vertex pair $X, Y \in V$, which are connected by an edge in E, also satisfies the equality in condition 2 for any other vertex pairs that are not connected by an edge.

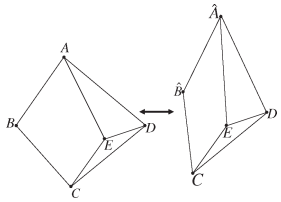

Fig. 2. Discontinuous flex ambiguity. By removing the edge AD, flexing the edges AB, BC, and AE, and reinserting the edge AD, a different realization can be obtained while satisfying the same distance constraints.

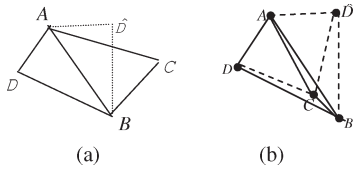

Fig. 3. (a) Flip ambiguity in a rigid but not globally rigid underlying graph. By reflecting D across the line connecting sensor nodes A and B, we obtain a new realization $\hat{D}$ satisfying the same distance constraints. (b) Flip ambiguity in a globally rigid underlying graph with a near-collinear neighborhood. Depending on the sensitivity of the near-collinear neighborhood ABC to the intersensor distance measurement errors, D can be estimated at a flipped location $\hat{D}$ satisfying approximately the same distance constraints.

B. Ambiguities in Sensor Network Localization

If a framework (G, p) is rigid but not globally rigid, there exist two types of discontinuous deformations that can prevent a representation of G from being consistent with p, i.e., a representation (G, p_1) satisfying $\|p(X) - p(Y)\| = \|p_1(X) - p_1(Y)\|$ for any vertex pair $X, Y \in V$, which are connected by an edge in E, from being unique (in the sense that it differs from other such representations at most by translation, rotation, or reflection) [15], [16]: flip and discontinuous flex ambiguities.

Discontinuous flex ambiguities arise when the removal of an edge or a set of edges allows the remaining part of the graph to be flexed continuously to a different realization while satisfying the same distance constraints when the removed edge(s) is (are) reinserted (see Fig. 2).

When an underlying graph is rigid but not globally rigid, a vertex (sensor node) of the underlying graph may have a set of neighbors forming a mirror across which the vertex (sensor node) can be reflected. Such a phenomenon is called a flip ambiguity, which is depicted in an example in Fig. 3(a).

However, even in a sensor network with a globally rigid underlying graph, a sensor node can still be reflected across its near-collinear neighbors depending on the sensitivity of the near-collinear neighborhood to the corresponding distance measurement errors [4]. Fig. 3(b) depicts an example of such situations. Thus, erroneous measured distances may cause flip ambiguities on near-collinear neighborhoods, depending on the sensitivity of those near-collinear neighborhoods to such measurement errors.

IV. Error-Propagation Effects of Flip Ambiguities

This section, using a simple example, describes how flip-ambiguity effects can propagate in a sequential or incremental

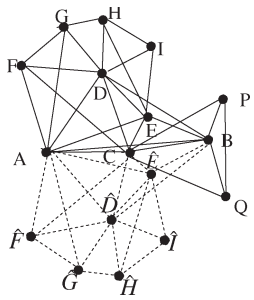

Fig. 4. Avalanche error propagation of a single flip ambiguity. Initially, the locations of A, B, C, P, and Q are known, and D, E, F, G, H, and I are unknown. At first, D and E uses the locations of near-collinear neighbors A, B, and C and localize themselves at $\hat{D}$ and $\hat{E}$ [satisfying (38)] due to flip ambiguity. Then, F uses the locations of neighbors A, C, and D and localizes itself at $\hat{E}$. Subsequently, G, H, and I will get localized at $\hat{G}$, $\hat{H}$, and $\hat{I}$, respectively. Here, a flip ambiguity in D (and E) caused nodes F, G, H, and I to have large estimation errors.

localization [22], [23], [30]–[32]. A similar explanation of flip-ambiguity effects in a cluster localization followed by stitching/patching [15], [24], [33]–[35] can be found in [18]. For convenience, we call a sensor with *a priori* known location or whose location has already been estimated as an anchor or a known sensor node and a sensor with unknown location as an unknown sensor node.

In a sequential localization algorithm [22], [23], [30]–[32], unknown sensor nodes are localized once they have three or more known neighbors. As soon as a sensor node is localized, it will be elevated to have anchor status, increasing the number of known neighbors of some unknown sensor nodes and may make them eligible for localization. Sequential localization continues until there are no unknown sensor nodes with at least three known neighbors. Flip ambiguity in any location estimate may cause an avalanche effect in the subsequent location estimates, thereby causing large estimation errors. Such a phenomenon is demonstrated in Fig. 4 via a simple example. We call the aforementioned kind of error propagation as *avalanche error propagation*, where the estimation error multiplication allows very large estimation errors to propagate in the network starting with the flipped realization of a single node. The error-propagation effects, where the location estimation error increases with the sequence of location estimates, become apparent in sequential localization algorithms when the number of anchors is small.

From the aforementioned illustration, we can see that when a flip ambiguity occurs, it may drastically corrupt the sensor network localization or, in the extreme case, may even make the whole network localization collapse. Hence, it is necessary to identify the possible occurrence of flip ambiguity in any neighborhood to avoid large localization errors. Finally, we also want to point out that such avalanche error-propagation phenomenon also exists in centralized localization algorithms, as shown in Fig. 1 and [8].

The robustness criterion proposed in Section VI can be used by localization algorithms to make a binary decision of whether to accept or to reject a neighbor node being considered as a member of a neighborhood in a localization process. To keep the analysis simple, the robustness criterion is formed only by considering *fully connected quadrilaterals* (FCQs), which are quadruples of sensor nodes, all of which are neighbors of each other, i.e., the distance between any pair is measurable. In the localization process, a robust neighbor set $RN_X \subset N_X$ is formed for every unknown sensor node X by selecting all members $Y \in N_X$ that do not contribute to flip ambiguity, using the robustness criterion. Hence, the robustness criterion helps the localization algorithm to use information from all known neighbors that do not contribute to flip ambiguity.

V. Quantitative Analysis of Flip Ambiguities

This section analyzes the conditions under which a flip ambiguity is likely to occur in an arbitrary FCQ of a given sensor network. The analysis assumes a disc transmission model of radius R around each sensor node X.

Assumption 1: Two sensor nodes X and Y are said to be neighbors of each other and are able to measure their intersensor distance to each other if and only if the true distance $|XY| \leq R$. In accordance with this disc transmission model, any intersensor distance measurement $\overline{d}_{XY} > R$ is assumed to be truncated to R.

Furthermore, as justified in [36], this analysis uses a Gaussian distribution with zero mean and a standard deviation of σ as the noise model for the distance measurement errors. Thus, it is possible to state that the absolute value of the distance measurement error is smaller than a *threshold* $\overline{\epsilon} > 0$ with a certain probability. To keep this probability high, $\overline{\epsilon}$ can be chosen as 3σ, such that the probability of the absolute value of the distance measurement error being less than $\overline{\epsilon}$ is 99%. Based on this observation, we consider a truncated version of the Gaussian distribution and state the following assumption.

Assumption 2: For every neighbor node pair $X, Y \in N_X$, the difference between the true distance $|XY|$ and the measured distance $\overline{d}_{XY}$ is within a known value $\overline{\epsilon} > 0$, i.e.,

$$\left| |XY| - \overline{d}_{XY} \right| \leq \overline{\epsilon}. \tag{1}$$

In a localization problem, once the positions of three sensor nodes in an FCQ are precisely known and the measurements of the distances of the fourth sensor node from each of these three sensor nodes are available, the fourth sensor node is localizable. Consider an *ordered FCQ* $ABCD$ as a quadruple of sensor nodes A, B, C, and D, where the locations of A, B, and C are known together with intersensor distance measurements $\overline{d}_{AD}$, $\overline{d}_{BD}$, and $\overline{d}_{CD}$. The localization task focuses on the particular problem of estimating the location of sensor node D using the given fixed positions of neighbor nodes A, B, and C and intersensor measurements $\overline{d}_{AD}$, $\overline{d}_{BD}$, and $\overline{d}_{CD}$.

Following the notation in parallel with [15] and [26], an FCQ is called $(\overline{\epsilon}, \delta_S)$-*robust* (with respect to distance measurement errors) if the fourth sensor node (called sensor node D) is uniquely localizable with a predefined accuracy level $\delta_S > 0$ when the corresponding absolute measurement errors are less than a predefined threshold $\overline{\epsilon} > 0$.

The analysis is started with the focus on the following generic localization method.

Step 1) Using $\overline{d}_{AD}$ and $\overline{d}_{BD}$ only, find the two possible locations $\hat{D}$ and $\hat{D}'$ for sensor node D as intersection points of the circles $\mathcal{C}(A, \overline{d}_{AD})$ with center A and radius $\overline{d}_{AD}$ and $\mathcal{C}(B, \overline{d}_{BD})$ with center B and radius $\overline{d}_{BD}$. These two points $\hat{D}$ and $\hat{D}'$ are symmetrical with respect to AB.

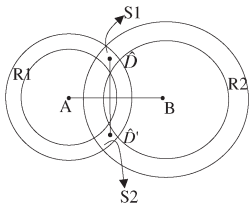

Fig. 5. Two regions S_1 and S_2 for the possible location-estimation pair $(\hat{D}, \hat{D}')$ defined by the intersection of the two rings R_1 and R_2 represented by (4) and (5).

Step 2) Using the third distance measurement $\overline{d}_{CD}$, decide on which of $\hat{D}$ and $\hat{D}'$ to choose as the location estimate of D that better matches the distance constraints.

Remark 1: Without loss of generality, the aforementioned processing order of the intersensor measurements $(\overline{d}_{AD}, \overline{d}_{BD}, \overline{d}_{CD})$ is chosen, but the analysis below can easily be adapted to any other order of distance measurements.

This generic localization method does not consider the distance measurement errors in $\overline{d}_{AD}$ and $\overline{d}_{BD}$. Using Assumption 2, for a given $\overline{\epsilon}$, the erroneous measured distances $\overline{d}_{AD}$, $\overline{d}_{BD}$, and $\overline{d}_{CD}$ can be bounded using the true distances $|AD|$, $|BD|$, and $|CD|$ as

$$\overline{d}_{XD} \in [\,|XD| - \overline{\epsilon}, |XD| + \overline{\epsilon}\,], \qquad \forall\, X \in \{A, B, C\}. \tag{2}$$

Equivalently

$$|XD| \in [\,\overline{d}_{XD} - \overline{\epsilon}, \overline{d}_{XD} + \overline{\epsilon}], \qquad \forall\, X \in \{A, B, C\}. \tag{3}$$

A. Analysis of Flip Ambiguities Using a Particular Distance Measurement Pair $\overline{d}_{AD}$ and $\overline{d}_{BD}$

In this section, the criterion for flip ambiguity is analyzed using the erroneous distance measurements of sensor node D from neighbors A and B first. In the presence of distance measurement errors in $\overline{d}_{AD}$ and $\overline{d}_{BD}$, the possible locations $\hat{D}$ and $\hat{D}'$ of sensor node D are inside the two regions S_1 and S_2 (see Fig. 5), which are the intersection of the two rings R_1 and R_2 defined as

$$\begin{aligned} R_1 = \big\{(x,y)\,|\,(\,\overline{d}_{AD} - \overline{\epsilon}\,)^2 &\le (x - x_A)^2 + (y - y_A)^2 \\ &\le (\,\overline{d}_{AD} + \overline{\epsilon}\,)^2\big\} \end{aligned} \tag{4}$$

$$\begin{aligned} R_2 = \big\{(x,y)\,|\,(\,\overline{d}_{BD} - \overline{\epsilon}\,)^2 &\le (x - x_B)^2 + (y - y_B)^2 \\ &\le (\,\overline{d}_{BD} + \overline{\epsilon}\,)^2\big\} \end{aligned} \tag{5}$$

where (x_A, y_A) and (x_B, y_B) are the known coordinates of sensor nodes A and B, respectively. Here, the points $\hat{D}$ and $\hat{D}'$, as well as the regions S_1 and S_2, are symmetrical with respect to AB.

The generic task of sensor localization is estimating the location of each sensor node such that the magnitude of the corresponding estimation error is less than or equal to a predefined accuracy level $\delta_S > 0$ when the corresponding absolute measurement errors are less than a predefined threshold $\overline{\epsilon} > 0$. Hence, an error caused by a flip ambiguity where $|\hat{D}\hat{D}'| < \delta_S$ is not substantial. In this paper, a flip ambiguity that does not cause a substantial error in the estimated location of a sensor is called a *negligible flip ambiguity*. Hence, a flip ambiguity is substantial if there exist a $\hat{D} \in S_1$ and a $\hat{D}' \in S_2$ symmetrical to $\hat{D}$ with respect to AB such that

$$\frac{1}{2}\left|\,|C\hat{D}| - |C\hat{D}'|\,\right| \le \overline{\epsilon} \quad \text{when } |\hat{D}\hat{D}'| > \delta_S. \tag{6}$$

Hence, the criterion to judge the $(\overline{\epsilon}, \delta_S)$-robustness of an FCQ can be stated as

$$\min_{\substack{\hat{D}\in S_1 \\ \hat{D}'\text{symmetrical to } \hat{D} \text{ w.r.t. } AB}} \frac{1}{2}\left|\,|C\hat{D}| - |C\hat{D}'|\,\right| > \overline{\epsilon} \quad \text{when } |\hat{D}\hat{D}'| > \delta_S \tag{7}$$

for a given neighborhood of A, B, C and measured distances $\overline{d}_{AD}$ and $\overline{d}_{BD}$. Note that the three distance measurement errors in $\overline{d}_{AD}$, $\overline{d}_{BD}$, and $\overline{d}_{CD}$ are simultaneously considered in (7). Distance measurement errors in $\overline{d}_{AD}$ and $\overline{d}_{BD}$ determine the regions S_1 and S_2, and the minimization of $(1/2)(\|C\hat{D}| - |C\hat{D}'\|)$ over these regions means that (7) considers the errors in both $\overline{d}_{AD}$ and $\overline{d}_{BD}$. The error in $\overline{d}_{CD}$ is explicitly considered in the inequality in (7).

B. Analysis of Flip Ambiguities Using Any Pair of Distance Measurements $\overline{d}_{AD}$, $\overline{d}_{BD}$, and $\overline{d}_{CD}$

The aforementioned analysis analyzed the criterion for flip ambiguities using the distance measurements of sensor node D from neighbor nodes A and B first to form the regions S_1 and S_2. If instead, the distance measurements of sensor node D from neighbor nodes A and C are considered first, the two possible locations $\hat{D}$ and $\hat{D}'$ of sensor node D will be inside two different regions S_1^{AC} and S_2^{AC} symmetrical with respect to AC, leading to a different robustness criterion

$$\min_{\substack{\hat{D}\in S_1^{AC} \\ \hat{D}' \text{ symmetrical to } \hat{D} \text{ w.r.t. } AC}} \frac{1}{2}\left|\,|B\hat{D}| - |B\hat{D}'|\,\right| > \overline{\epsilon} \quad \text{when } |\hat{D}\hat{D}'| > \delta_S. \tag{8}$$

Hence, the criterion to judge the $(\overline{\epsilon}, \delta_S)$-robustness of an FCQ $ABCD$ should satisfy all three permutations of the sequence A, B, and C as stated as follows:

$$\min_{\substack{\hat{D}\in S_1^{XY} \\ \hat{D}' \text{ symmetrical to } \hat{D} \text{ w.r.t. } XY \\ X,Y,Z\in\{A,B,C\}, X\neq Y\neq Z}} \frac{1}{2}\left|\,|Z\hat{D}| - |Z\hat{D}'|\,\right| > \overline{\epsilon} \quad \text{when } |\hat{D}\hat{D}'| > \delta_S. \tag{9}$$

VI. Identification of Possible Flip Ambiguities

A. Identification of Flip Ambiguities Using a Particular Distance Measurement Pair $\overline{d}_{AD}$ and $\overline{d}_{BD}$

This section focuses on the minimum of the flip-ambiguity indicator $||C\hat{D}| - |C\hat{D}'||$ and formulates a robustness criterion of FCQs $ABCD$ while using the distance measurements of sensor node D from neighbors A and B first. Without loss of

generality, let the coordinates of A and B lie on the x-axis with the midpoint of AB at the origin. Then, $(-x_B, 0)$ and $(x_B, 0)$ are the coordinates of A and B, respectively, where $x_B = |AB|/2$. Let (x_C, y_C) be the coordinate of sensor node C. With these definitions, (4) and (5) can be rewritten as

$$R_1 = \left\{(x,y) \,|\, (\overline{d}_{AD} - \overline{\epsilon})^2 \le (x + x_B)^2 + y^2 \le (\overline{d}_{AD} + \overline{\epsilon})^2\right\} \quad (10)$$

$$R_2 = \left\{(x,y) \,|\, (\overline{d}_{BD} - \overline{\epsilon})^2 \le (x - x_B)^2 + y^2 \le (\overline{d}_{BD} + \overline{\epsilon})^2\right\}. \quad (11)$$

Without loss of generality, let the location (x, y) of $\hat{D}$ be in S_1 and the location $(x, -y)$ of $\hat{D}'$ be in S_2, where S_1 and S_2 are defined using (10) and (11) as

$$S_1 = \{(x,y) \,|\, (x,y) \in (R_1 \cap R_2)\} \text{ and } y > 0 \quad (12)$$

$$S_2 = \{(x,-y) \,|\, (x,-y) \in (R_1 \cap R_2)\} \text{ and } y > 0. \quad (13)$$

The regions S_1 and S_2 are considered to be disjoint in the initial analysis.

If an error function e is defined as

$$e \triangleq \left| |C\hat{D}| - |C\hat{D}'| \right| \quad (14)$$

then (7) can be written as

$$\min_{\substack{\hat{D} \in S_1 \\ \hat{D}' \text{ symmetrical to } \hat{D} \text{ w.r.t. } AB}} e^2 > 4\overline{\epsilon}^2 \text{ when } |\hat{D}\hat{D}'| > \delta_S. \quad (15)$$

From (12), (13), and Fig. 6, it is seen that when (x_S, y_S), (x_Q, y_Q), (x_R, y_R), and (x_P, y_P) are the coordinates of the intersection points S, Q, R, and P, respectively, then the range of the coordinates (x, y) and $(x, -y)$ of $\hat{D}$ and $\hat{D}'$, respectively, satisfying (12) and (13), is bounded as follows:

$$x_S \le x \le x_Q \quad \text{and} \quad y_P \le y \le y_R. \quad (16)$$

To further analyze (15), let us write $|C\hat{D}|$ and $|C\hat{D}'|$ in terms of the coordinates of C, $\hat{D}$, and $\hat{D}'$ as $|C\hat{D}| = \sqrt{(x_C - x)^2 + (y_C - y)^2}$ and $|C\hat{D}'| = \sqrt{(x_C - x)^2 + (y_C + y)^2}$, giving (17), shown at the bottom of the page.

From (17), we can see that for a fixed y, e^2 is minimized when $|x - x_C|$ is maximized. Depending on the location of sensor node C, the minimum of e^2 will occur when either $\hat{D}$ is on the left boundary of S_1 (arcs RS and SP in Fig. 6) or $\hat{D}$ is on the right boundary of S_1 (arcs RQ and QP in Fig. 6). If sensor node C is on the right side of the region, i.e., closer to the right boundary of S_1 than to the left boundary, the minimum will occur when $\hat{D}$ is on the left boundary of S_1; otherwise, the minimum will occur when $\hat{D}$ is on the right boundary of S_1. This can also be shown by examining the partial derivative of e^2. If we take the partial derivative of e^2 with respect to x

$$\frac{\partial e^2}{\partial x} = 4(x_C - x)\left(\frac{(x_C - x)^2 + y_C^2 + y^2}{\sqrt{\left((x_C - x)^2 + y_C^2 + y^2\right)^2 - 4y_C^2 y^2}} - 1\right). \quad (18)$$

Since

$$\left((x_C - x)^2 + y_C^2 + y^2\right)^2 - 4y_C^2 y^2 = (x_C - x)^4 + 2(x_C - x)^2\left(y_C^2 + y^2\right) + \left(y_C^2 - y^2\right)^2 > 0$$

the value of $\sqrt{((x_C - x)^2 + y_C^2 + y^2)^2 - 4y_C^2 y^2}$ is always real. A closer look reveals that

$$\sqrt{\left((x_C - x)^2 + y_C^2 + y^2\right)^2 - 4y_C^2 y^2} = 2|C\hat{D}||C\hat{D}'| \quad (19)$$

which is a product of two distances, and hence

$$\sqrt{\left((x_C - x)^2 + y_C^2 + y^2\right)^2 - 4y_C^2 y^2} > 0.$$

Moreover

$$\sqrt{\left((x_C - x)^2 + y_C^2 + y^2\right)^2 - 4y_C^2 y^2} < \sqrt{\left((x_C - x)^2 + y_C^2 + y^2\right)^2} = (x_C - x)^2 + y_C^2 + y^2.$$

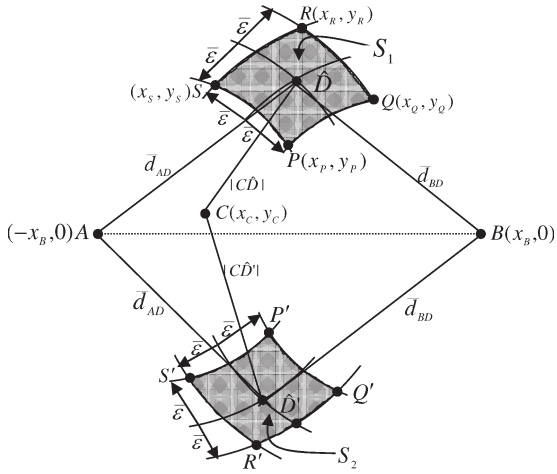

Fig. 6. Detailed illustration of the two regions S_1 and S_2 and the possible location-estimation pair $(\hat{D}, \hat{D}')$ using the accurate locations of sensor nodes A and B, erroneous intersensor distance measurements $\overline{d}_{AD}$ and $\overline{d}_{BD}$, and the threshold value $\overline{\epsilon}$.

$$e^2 = \left(|C\hat{D}| - |C\hat{D}'|\right)^2 = 2\left((x_C - x)^2 + y_C^2 + y^2 - \sqrt{\left((x_C - x)^2 + y_C^2 + y^2\right)^2 - 4y_C^2 y^2}\right) = \frac{8y_C^2 y^2}{(x_C - x)^2 + y_C^2 + y^2 + \sqrt{\left((x_C - x)^2 + y_C^2 + y^2\right)^2 - 4y_C^2 y^2}} \quad (17)$$

It follows that

$$1 < \frac{(x_C - x)^2 + y_C^2 + y^2}{\sqrt{\left((x_C - x)^2 + y_C^2 + y^2\right)^2 - 4y_C^2 y^2}}$$

and hence

$$0 < \left(\frac{(x_C - x)^2 + y_C^2 + y^2}{\sqrt{\left((x_C - x)^2 + y_C^2 + y^2\right)^2 - 4y_C^2 y^2}} - 1 \right)$$

enforcing that there is only one extremum for e^2, which is at $x = x_C$. It is also seen from (18) that e^2 is an increasing function (i.e., $\partial e^2/\partial x > 0$) when $x < x_C$ and a decreasing function (i.e., $\partial e^2/\partial x < 0$) when $x > x_C$. This leads to the conclusion that, for any fixed value of y, the minimum of e^2 when $\hat{D} \in S_1$ occurs at the boundaries of S_1 where $|x_C - x|$ is at its maximum. Rewriting the squared error term e^2 as in (20), shown at the bottom of the page, we get

$$\lim_{y \to +\infty} e^2 = 4y_C^2 \quad \lim_{y \to 0} e^2 = 0 \text{ for any fixed value of } x.$$

For any fixed x, when y decreases, e^2 also decreases. Given the condition that $y_P \leq y \leq y_R$, it can be concluded that irrespective of the location of sensor node C, for any fixed x, the minimum of e^2 will occur when $\hat{D}$ is on the lower boundary (arcs SP and PQ in Fig. 6) of S_1. This conclusion can also be obtained by examining the partial derivative of e^2.

From the aforementioned discussion, we can establish that the minimum of e^2 will only occur when $\hat{D}$ is on the lower boundary of S_1. When C is on the right side of S_1, the minimum occurs when $\hat{D}$ is on the lower left boundary of S_1 (arc SP in Fig. 6); likewise, when C is on the left side of S_1, i.e., closer to the left boundary of S_1 than to the right boundary, the minimum occurs when $\hat{D}$ is on the lower right boundary of S_1 (arc QP in Fig. 6). Without loss of generality let us focus on the case when C is on the right side of S_1, and hence, the minimum of e^2 occurs when D is on the lower left boundary of S_1, i.e., when $\hat{D}$ is on the segment SP. In the following paragraph, we shall further narrow down the range of $\hat{D}$ and establish that the minimum of e^2 will only occur when $\hat{D}$ is either at point S or at point P.

Since arc SP is a part of the circle centered at $(-x_B, 0)$ with a radius $\overline{d}_{AD} - \overline{\epsilon}$, when $\hat{D}$ is on the segment SP, we can obtain the following relationship between y and x:

$$y^2 = (\overline{d}_{AD} - \epsilon)^2 - (x + x_B)^2.$$

Substituting this relationship of x and y into e^2 in (17), it has the form shown in (21), shown at the bottom of the page.

Equations (22) and (24), shown at the bottom of the page, show the first derivative of e^2 with respect to x and the second derivative of e^2 with respect to x [obtained using $\partial(U/V)/\partial x$, where U and V are as in (23), shown at the bottom of the page],

$$e^2 = \frac{8y_C^2}{\frac{\left((x_C - x)^2 + y_C^2\right)}{y^2} + 1 + \sqrt{\frac{\left((x_C - x)^2 + y_C^2\right)^2}{y^4} + \frac{2\left((x_C - x)^2 - y_C^2\right)}{y^2} + 1}} \tag{20}$$

$$\begin{aligned} e^2 &= 2\left((x_C - x)^2 + y_C^2 + y^2 - \sqrt{\left((x_C - x)^2 + y_C^2 + y^2\right)^2 - 4y_C^2 y^2} \right) \\ &= 2\Bigg((x_C - x)^2 - (x_B + x)^2 + y_C^2 + (\overline{d}_{AD} - \overline{\epsilon})^2 \\ &\qquad - \sqrt{\left((x_C - x)^2 - (x_B + x)^2 + y_C^2 + (\overline{d}_{AD} - \overline{\epsilon})^2\right)^2 + 4y_C^2(x_B + x)^2 - 4y_C^2(\overline{d}_{AD} - \overline{\epsilon})^2} \Bigg) \end{aligned} \tag{21}$$

$$\frac{\partial(e^2)}{\partial x} = -4\left((x_C + x_B) - \frac{\left(x_C^2 - 2x(x_C + x_B) - x_B^2 + y_C^2 + (\overline{d}_{AD} - \overline{\epsilon})^2\right)(x_C + x_B) - 2y_C^2(x_B + x)}{\sqrt{\left(x_C^2 - 2x(x_C + x_B) - x_B^2 + y_C^2 + (\overline{d}_{AD} - \overline{\epsilon})^2\right)^2 + 4y_C^2(x_B + x)^2 - 4y_C^2(\overline{d}_{AD} - \overline{\epsilon})^2}} \right) \tag{22}$$

$$U = \left(x_C^2 - 2x(x_C + x_B) - x_B^2 + y_C^2 + (\overline{d}_{AD} - \overline{\epsilon})^2\right)(x_C + x_B) - 2y_C^2(x_B + x)$$

$$V = \sqrt{\left(x_C^2 - 2x(x_C + x_B) - x_B^2 + y_C^2 + (\overline{d}_{AD} - \overline{\epsilon})^2\right)^2 + 4y_C^2(x_B + x)^2 - 4y_C^2(\overline{d}_{AD} - \overline{\epsilon})^2} \tag{23}$$

$$\frac{\partial^2(e^2)}{\partial x^2} = \frac{-8y_C^2\left((\overline{d}_{AD} - \overline{\epsilon})^2 - \left((x_C + x_B)^2 + y_C^2\right)\right)^2}{(V)^{\frac{3}{2}}} \tag{24}$$

respectively. From (17) and (21), it can easily be seen that $V = |C\hat{D}||C\hat{D}'| > 0$. Hence, (24) shows that the second derivative of e^2 is always negative, i.e., e^2 is a concave function of x when $\hat{D}$ is confined to the segment SP. The property of the concave function readily leads to the conclusion that when $\hat{D}$ is on the segment SP, the minimum of e^2 occurs only at the boundaries, i.e., when $\hat{D}$ is either at point S or at point P.

Following the same analysis in the last paragraph, it can be established that when C is on the left side of S_1, the minimum of e^2 occurs only when $\hat{D}$ is either at point P or at point Q. In summary, through the earlier discussions, we have established that the minimum of e^2 for $\hat{D} \in S_1$ is achieved only when $\hat{D}$ is at one of the three boundary points S, Q, or P of S_1. Hence, the robustness criterion (15) can be rewritten as

$$\min_{\substack{\hat{D}\in\{S,Q,P\} \\ \hat{D}' \text{ symmetrical to } \hat{D} \text{ w.r.t. } AB}} e^2 \triangleq \left(|C\hat{D}| - |C\hat{D}'|\right)^2 > 4\bar{\epsilon}^2 \quad \text{when } |\hat{D}\hat{D}'| > \delta_S. \tag{25}$$

B. Identification of Flip Ambiguities Using Any Pair of Distance Measurements $\overline{d}_{AD}$, $\overline{d}_{BD}$, and $\overline{d}_{CD}$

The aforementioned analysis analyzed the minimum of $e^2 = (|C\hat{D}| - |C\hat{D}'|)^2$ for $\hat{D} \in S_1$ while using the distance measurements of sensor node D from neighbors A and B first. If, instead, the distance measurements of sensor node D from neighbors A and C are considered first in finding the minimum of $e^2 = (|B\hat{D}| - |B\hat{D}'|)^2$, then $\hat{D}$ will be symmetric to $\hat{D}'$ with respect to AC, and the confined regions S_1 and S_2 (together with the intersection points S, P, and Q) will be determined by the measured distances $\overline{d}_{AD}$ and $\overline{d}_{CD}$ and the threshold $\bar{\epsilon}$. The intersection points S, P, and Q with respect to AC (let them be S^{AC}, P^{AC}, and Q^{AC}) will be different from their counterparts with respect to AB (i.e., S^{AB}, P^{AB}, and Q^{AB}), leading to varying minimum values of e^2. Hence, the minimum e^2 for all three permutations of the sequence A, B, and C should be

$$\min_{\substack{\hat{D}\in\{S^{XY},Q^{XY},P^{XY}\} \\ \hat{D}' \text{ symmetrical to } \hat{D} \text{ w.r.t. } XY \\ X,Y,Z\in\{A,B,C\}, X\neq Y\neq Z}} e^2 \triangleq \left(|Z\hat{D}| - |Z\hat{D}'|\right)^2 > 4\bar{\epsilon}^2 \quad \text{when } |\hat{D}\hat{D}'| > \delta_S. \tag{26}$$

The results of our analysis in this section are summarized in the following propositions.

Proposition 1: Given fixed positions A, B, and C and for given measurements $\overline{d}_{AD}$, $\overline{d}_{BD}$, and $\overline{d}_{CD}$ satisfying $\delta_S/2 < \overline{d}_{AD}, \overline{d}_{BD}, \overline{d}_{CD} \leq R$, if there are two disjoint regions S_1 and S_2 defined by (12) and (13), then the minimum of e^2 in (15) occurs at S, P or Q, where S, P, and Q are defined right before (16) and illustrated in Fig. 5.

Proposition 2: For given fixed positions A, B, and C and for given measurements $\overline{d}_{AD}$, $\overline{d}_{BD}$, and $\overline{d}_{CD}$ satisfying $\delta_S/2 < \overline{d}_{AD}, \overline{d}_{BD}, \overline{d}_{CD} \leq R$, the quadrilateral $ABCD$ satisfying (26) does not suffer from substantial flip ambiguity.

The aforementioned analysis only considered the situation in which the two regions S_1 and S_2 are disjoint. If instead they are joint, as shown in Fig. 7, the minimum of e^2 will always

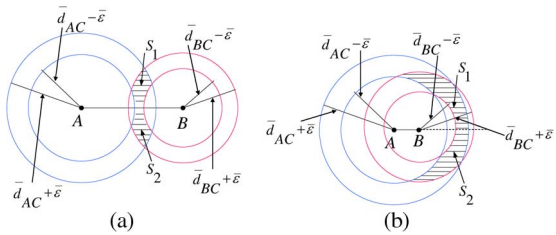

Fig. 7. Examples of joint regions S_1 and S_2. (a) Circles $\mathcal{C}(A, \overline{d}_{AC} - \bar{\epsilon})$ and $\mathcal{C}(B, \overline{d}_{BC} - \bar{\epsilon})$ do not intersect, causing S_1 to be joint to S_2. (b) Circles $\mathcal{C}(A, \overline{d}_{AC} - \bar{\epsilon})$ and $\mathcal{C}(B, \overline{d}_{BC} + \bar{\epsilon})$ do not intersect, causing S_1 to be joint to S_2.

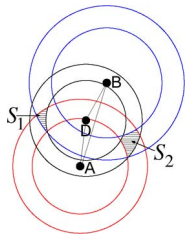

Fig. 8. More precisely defined two regions S_1 and S_2 for the possible location estimation pair $(\hat{D}, \hat{D}')$ of sensor node D using the accurate locations of sensor nodes A, B, and C and intersensor distance measurements $\overline{d}_{AD}$, $\overline{d}_{BD}$, and $\overline{d}_{CD}$. Here, S_1 and S_2 are the intersection of the three rings R_1, R_2, and R_3 defined by (27)–(29).

be zero when $\hat{D}$ and $\hat{D}'$ both coincide at the same point on the common boundary of S_1 and S_2. In such situations, the FCQs will always be detected as not robust. This scenario can happen more frequently when either the noise in the distance measurement is large or the chosen threshold $\bar{\epsilon}$ is large and may cause an increase in false alarms.

C. Identification of Flip Ambiguities When Regions S_1 and S_2 Are Considered Nonsymmetrical

The robustness criterion (25) formulated in Section VI-A considers $\hat{D}$ and $\hat{D}'$ to be symmetric to the line AB. This assumption is reasonable while considering that the regions S_1 and S_2 are formed by the constraints imposed by two neighboring sensors A and B. Instead, if all three constraints imposed by the three neighboring sensors A, B, and C are considered, the possible regions S_1 and S_2 for the possible location pair $(\hat{D}, \hat{D}')$ will be formed by the intersection of the three rings defined by

$$R_1 = \left\{(x,y) \,|\, (\overline{d}_{AD} - \bar{\epsilon})^2 \leq (x - x_A)^2 + (y - y_A)^2 \leq (\overline{d}_{AD} + \bar{\epsilon})^2\right\} \tag{27}$$

$$R_2 = \left\{(x,y) \,|\, (\overline{d}_{BD} - \bar{\epsilon})^2 \leq (x - x_B)^2 + (y - y_B)^2 \leq (\overline{d}_{BD} + \bar{\epsilon})^2\right\} \tag{28}$$

$$R_3 = \left\{(x,y) \,|\, (\overline{d}_{CD} - \bar{\epsilon})^2 \leq (x - x_C)^2 + (y - y_C)^2 \leq (\overline{d}_{CD} + \bar{\epsilon})^2\right\} \tag{29}$$

and are more likely to be nonsymmetrical. An example of nonsymmetrical regions S_1 and S_2 is shown in Fig. 8.

Let H_C denote the open half-plane with border line AB that contains C and $H_{\overline{C}}$ be the complementary half-plane on the

other side of AB. Without loss of generality, let $S_1 \subset H_C$, which makes $S_2 \subset H_{\overline{C}}$. Thus, S_1 and S_2 can be redefined as

$$S_1 = \{(x,y) \,|\, (x,y) \in (R_1 \cap R_2 \cap R_3 \cap H_C)\} \quad (30)$$
$$S_2 = \left\{(x,y) \,|\, (x,y) \in (R_1 \cap R_2 \cap R_3 \cap H_{\overline{C}})\right\}. \quad (31)$$

Note that the true location D lies in only one of the two regions S_1 or S_2, and thus, one of them always exist. Depending on the known locations of A, B, and C, the corresponding distance measurements $\overline{d}_{AD}$, $\overline{d}_{BD}$, and $\overline{d}_{CD}$, and the threshold $\overline{\epsilon}$, the other region may or may not exist. With these definitions and analysis, the robustness criterion (25) can be redefined as

$$\min_{\hat{D}\in S_1, \hat{D}'\in S_2} e^2 \triangleq \left(|C\hat{D}| - |C\hat{D}'|\right)^2 > 4\overline{\epsilon}^2 \quad \text{when } |\hat{D}\hat{D}'| > \delta_S. \quad (32)$$

To generalize, when $X, Y, Z \in \{A, B, C\}$ and $X \neq Y \neq Z$, let H_Z denote the open half-plane with border line XY that contains Z, and let $H_{\overline{Z}}$ be the complementary half-plane on the other side of XY. Thus, S_Z and $S_{\overline{Z}}$ can be defined as

$$S_Z = \{(x,y) \,|\, (x,y) \in (R_1 \cap R_2 \cap R_3 \cap H_Z)\} \quad (33)$$
$$S_{\overline{Z}} = \left\{(x,y) \,|\, (x,y) \in (R_1 \cap R_2 \cap R_3 \cap H_{\overline{Z}})\right\} \quad (34)$$

and the consideration of minimum e^2 for all three permutations of the sequence A, B, and C will change (32) as follows:

$$\min_{\substack{\hat{D}\in S_Z, \hat{D}'\in S_{\overline{Z}} \\ X,Y,Z\in\{A,B,C\}, X\neq Y\neq Z}} e^2 \triangleq \left(|Z\hat{D}| - |Z\hat{D}'|\right)^2 > 4\overline{\epsilon}^2 \quad \text{when } |\hat{D}\hat{D}'| > \delta_S. \quad (35)$$

Finding a closed-form solution for (35) is a complex problem. Instead, a constrained minimization can be applied to evaluate (35) for any sensor quadruple $ABCD$. Since the robustness criterion is more likely to be applied on every sensor quadruple in a localization algorithm, a robustness criterion without a closed-form solution is not suitable for sensor network localization.

VII. Numerical Analysis of the Robustness Criterion

This section tests and compares the performance of different robustness criteria in detecting the possible flip ambiguities in the localization of sensor quadruples. In this numerical study, a pool of $|N_X|$-node sensor networks is created by uniformly distributing $|N_X|(=4)$ neighbors in a rectangular region of 100 m $\times$ 100 m with a transmission range of $R = 10$ m. Following Assumption 1 in Section V, two sensor nodes X and Y are said to be neighbors if and only if their intersensor distance is less than or equal to the transmission range R. The measured distance between any neighboring sensor node pair is obtained by blurring the intersensor distance with a Gaussian noise [36] of zero mean and variance σ^2 as

$$\overline{d}_{XY} = \overline{d}_{YX} = |XY| + \mathcal{N}(0, \sigma^2). \quad (36)$$

Since the distances are always positive, the Gaussian noise is truncated such that $0 \leq \overline{d}_{XY}$.

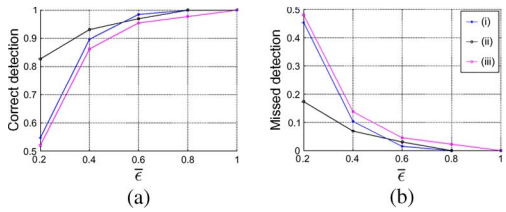

Fig. 9. (a) Ratio of correct flip detection to all the flip occurrences. (b) Ratio of missed flip detection to all the flip occurrences.

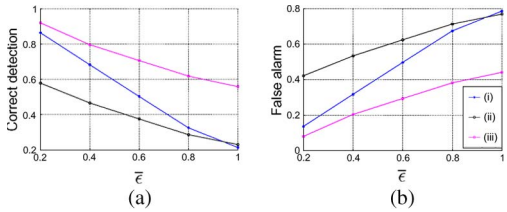

Fig. 10. (a) Ratio of correct detection when there is no flip ambiguity to all the occurrences of estimation without flip ambiguities. (b) Ratio of false alarm as flipped realization when there is no flip ambiguity to all the occurrences of estimation without flip ambiguities.

To compare different scenarios, various simulations are done with different pools of $|N_X|$-sensor networks created by varying the standard deviation of the Gaussian noise in (36) from 0.05 to 0.5 m. In each simulation, 10 000 FCQs are randomly selected from each pool of $|N_X|$-sensor networks, and localization is done by minimizing the cost function (38). To compare different scenarios, the same set of simulations are done with three different robustness criteria:

i) using robustness criterion (26);
ii) using the robustness criterion in [15];
iii) using robustness criterion (35).

The first set of simulations tested the effect of different thresholds on criteria (25) and (32) in detecting the flip ambiguities while having a fixed noise level of $\sigma = 0.2$ m. A numerical study in [18] shows that the estimation error will be within a value of 20% of the transmission range R when there is no flip ambiguity, but when there is a flip ambiguity, the error will be much larger than that. Thus, to simplify the detection of flipped realization, any estimation error $> R/5$ is treated as having substantial flip ambiguity. The obtained results are shown in Figs. 9 and 10. Fig. 9(a) shows the ratio of correct flip detection to all flipped estimates, and Fig. 9(b) shows the ratio of missed flip detection to all flipped estimates. It can be seen from these two figures that the rate of correct flip detection increases while the rate of missed flip detection decreases with increasing value of $\overline{\epsilon}$. Fig. 10(a) shows the ratio of correct detection to all estimates without flip, and Fig. 10(b) shows the ratio of estimates without flip ambiguities false alarmed to be flipped estimates to all the estimates without flip ambiguities. These two figures show that if the threshold is increased, the false-alarm rate is also increased. This is due to more frequent joining of regions S_1 and S_2 with larger thresholds. The effect of different noise levels (σ) on the correct detection of flipped estimates or estimates with no flip ambiguity is also studied with a threshold of $\epsilon = 3\sigma$. The results are shown in Fig. 11.

The second set of simulations repeated the previous set of simulations while removing the dependence on the choice of

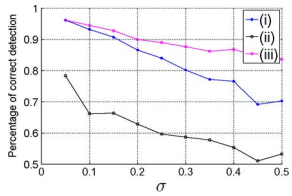

Fig. 11. Total number of correct detection against σ when the threshold is set as $\epsilon = 3\sigma$.

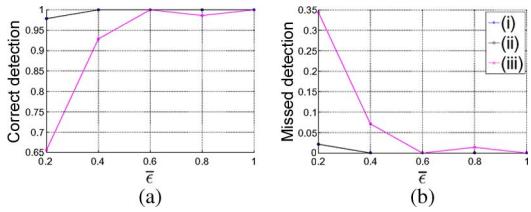

Fig. 12. (a) Ratio of correct flip detection to all the flip occurrences. (b) Ratio of missed flip detection to all the flip occurrences.

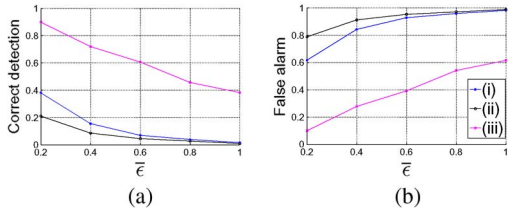

Fig. 13. (a) Ratio of correct detection when there is no flip to all the occurrences of estimation without flip. (b) Ratio of false alarm as flip when there is no flip to all the occurrences of estimation without flip.

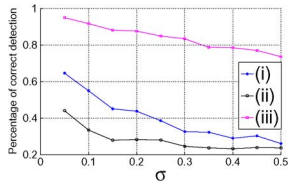

Fig. 14. Ratio of correct detection against σ when the threshold is set as $\epsilon = 3\sigma$.

the sequence of points A, B, and C in the analysis by using criteria (26) and (35) instead of (25) and (32).

Figs. 12 and 13 show the effect of different thresholds $(\bar{\epsilon})$ on the correct flip detection at a fixed noise level $(\sigma = 0.2$ m). Fig. 12(a) and (b) shows that when the dependence on the choice of the sequence of points A, B, and C is removed, the rate of correct flip detection is (almost) 100%, and the missed flip detection is (almost) 0% when the value $\bar{\epsilon} \geq 3\sigma$ (i.e., when the error bound is accurate). Fig. 13(a) and (b) shows that, with increasing threshold, the false-alarm rate gets higher. This is again due to more frequent joining of regions S_1 and S_2 with larger thresholds. Fig. 14 shows the effect of different noise levels σ on the correct detection of flip or no-flip ambiguity by (26) and (35) at a threshold $\bar{\epsilon}$ of 3σ. From Figs. 12–14, it can be seen that the robustness criterion (26) makes the correct decision more accurately than the robustness criterion in [15], where the assumption of symmetry is creating a considerable amount of false alarms compared with (35). The drawback of the criterion (26), as well as the criterion in [15], is that under conditions of high measurement noise, the algorithms may not be able to localize a significant number of sensor nodes. However, it has been well established that localization results will always be poor for sensor nodes that are not uniquely localizable, and it is better to eliminate these sensor nodes from the localization process [15], [17].

VIII. Performance Enhancement of Localization Algorithms Using the Robustness Criterion

This section enhances the performance of the localization algorithms mentioned in Section IV by applying the robustness criterion (26) in the neighborhood selection of the algorithms. Our robustness criterion (26) uses only the location and intersensor distance information of the neighbor node and can thus be used with any valid candidate, i.e., either one-hop or multihop neighbor, of the neighbor set N_D of each node D to be localized. However, to keep the simulation procedure simple, only one-hop neighbors are considered to be the valid candidates of neighbor set N_D.

The localization algorithms mentioned in Section IV use the neighbor set N_D to do either trilateration with any three members of N_D or multilateration with all members of N_D. In this paper, the three members of N_D for trilateration is selected using the robustness criterion (26) as follows: The neighbor set N_D is used to obtain sets $C_3^{|N_D|}$ of all possible FCQs with sensor nodes $A, B, C \in N_D$ and D and to find the most robust FCQ satisfying

$$\max_{\substack{A,B,C \in N_D \\ A \neq B \neq C \\ \text{FCQ } ABCD \text{ satisfy (26)}}} \; \min_{\substack{\hat{D} \in \{S^{XY}, Q^{XY}, P^{XY}\} \\ X,Y,Z \in \{A,B,C\}, X \neq Y \neq Z \\ \hat{D}' \text{ symmetrical to } \hat{D} \text{ w.r.t. } XY}} e^2 \triangleq \left(|Z\hat{D}| - |Z\hat{D}'| \right)^2 \tag{37}$$

to form the robust neighbor set RN_D to be used in trilateration.

In the case of mutilateration, the robust neighbor set RN_D is selected in a particular way as follows: First, the robust neighbor set RN_D is formed with the most robust FCQ as in trilateration. Then, every neighbor node $Y \in N_D \setminus RN_D$ is checked to see whether Y and D form a robust FCQ, together with every pair of sensor nodes in RN_D. If they do, then the robust neighbor set RN_D is enlarged as $RN_D := RN_D \cup Y$.

The next section give details of the use of the robustness criterion (26) in sequential localization algorithm and checks the performance enhancements via simulations. A similar study was done for a cluster-based localization algorithm, and the performance enhancement was noted to be similar to the sequential localization algorithm. To restrict the length of this paper, this algorithm and the simulation results are omitted in this paper.

A. Robustness Criterion in Sequential Localization

Algorithm: In a sequential (or incremental) localization algorithm, every unknown sensor node X checks how many of its known neighbors $Y \in N_X$ are eligible to be a member of the robust neighbor set RN_X. If they have at least three members in RN_X, they localize themselves, become elevated anchors, and broadcast their location information together with their elevated anchor status to all their neighbors $Y \in M_X$. On receiving elevated anchor status messages, an unknown sensor node updates its location-known neighbor set N_X. Before an unknown sensor node tries to localize itself each time, it checks

and processes any pending elevated anchor status messages. An unknown sensor node keeps trying to localize itself until either 1) it becomes an elevated anchor, or 2) it does receives no more elevated anchor messages. When all the unknown sensor nodes reach this state, the localization algorithm ends. At this point, there may be no sensor nodes localized due to RN_X having less than three anchors at the initial stage, or there may be one or more distinct clusters of sensor nodes localized. Irrespective of the number of localized clusters in the sensor network, all the localized sensor nodes are localized in the central coordinate system fixed by the anchor nodes.

Simulation Results: In applications like bushfire surveillance, water-quality surveillance, and precision irrigation, a large number of tiny sensors are randomly distributed over a large regular-shaped area and are stationary after being deployed. In such networks, a sequential algorithm is sufficient, and thus, the performance of both trilateration- and multilateration-based sequential localization algorithms is evaluated here via simulations, where the robust neighbor set RN_X is chosen using (26).

For a sensor network with a large number of sensor nodes, it is reasonable to assume the sensor distribution to be uniform, and such an assumption has widely been used in the area [5]–[7], [15], [22], [33]. Changing the sensor distribution method may only affect the frequency of collinear placement of sensor nodes. The focus of this paper is on identifying possible flip ambiguities by neighborhood geometries once the sensor nodes are placed and eliminating them from the localization process, and thus, this simulation only considers uniformly distributed sensor networks to demonstrate the performance enhancement. In the simulation, 500 different sensor networks are used, where different random seeds are used to populate each sensor network with 100 sensor nodes, which are uniformly distributed in a square region of 100 m $\times$ 100 m. In these 100 nodes, the first ten are chosen as anchor nodes and are initialized with random coordinates within the square region. The measured distance between any neighbor node pair is modeled using (36), where the standard deviation is chosen to be 0.2 m. The location of the unknown sensor nodes are estimated using

$$\hat{p}_{X^*} = \arg\min_{\hat{p}_X} \sum_{Y \in N_i} \left(\overline{d}_{XY} - \|\hat{p}_X - p_Y\| \right)^2 \qquad (38)$$

where $\hat{p}_X = (\hat{x}_X, \hat{y}_X)$ denotes any possible location estimate of sensor node X, $\overline{d}_{XY}$ is the measured distance between sensor nodes X and Y, and $N_X (\subseteq M_X)$ is the set of neighbors of X whose locations are known or already estimated in the localization process.

The average node degree is varied in the simulation from 4 to 25 by adjusting the transmission range while keeping the number of sensor nodes fixed. Fig. 15 shows the relationship of the average transmission range and the average node degree.

The average mean square error (MSE) in location estimates is calculated and normalized to the transmission range R as follows:

$$\text{MSE} = \frac{1}{|n|\{V_n \neq \emptyset\}|} \sum_{\substack{n=1 \\ |V_n| \neq 0}}^{500} \frac{\sum_{i \in V_n} (x_X - \hat{x}_X)^2 + (y_X - \hat{y}_X)^2}{|V_n| R^2}$$

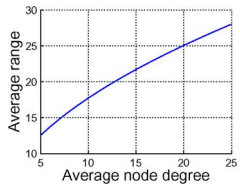

Fig. 15. Relationship of range versus average node degree.

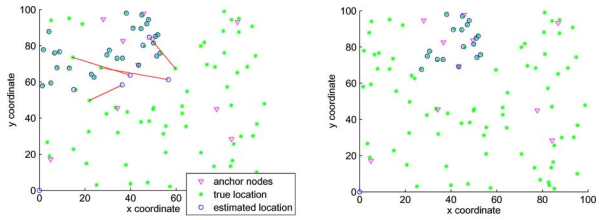

Fig. 16. Example of trilateration-based sequential localization having flip ambiguity and removal of such flip ambiguity by the robustness criterion. Multilateration-based sequential localization has similar performance in the removal of flip ambiguity. Here, the red line segments show the error offset between the original and the estimated location of the sensor node. (a) Localization without robustness criterion. (b) Localization with robustness criterion (26). It is worth noting here that, in this simulation, not many unknown sensor nodes have enough anchor nodes or elevated anchor nodes in their neighborhoods, resulting in an early termination of the sequential localization algorithm. Thus, only a small number of sensor nodes are localized. Since the total number of the sensor nodes is fixed in the simulations, the number of neighbors in a neighborhood is restricted by the transmission range, which is set to be 15 m in this case.

where $(\hat{x}_X, \hat{y}_X)$ and (x_X, y_X) are the estimated location and true location of sensor node X, and V_n is the set of sensor nodes localized in the nth sensor network, whereas $|V_n|$ is the number of sensor nodes in V_n.

The first set of simulations are done using a fixed threshold $\bar{\epsilon} = 3\sigma$ in the robustness criterion (26). To compare different scenarios, trilateration-based localization and multilateration-based localization are categorized into two groups, and the neighbors to be used in the location estimate of each group are chosen using three different methods:

A. trilateration
   - A.i) any three neighbors of N_X;
   - A.ii) three most robust neighbors of N_X by the criterion in [15];
   - A.iii) three most robust neighbors of N_X by criterion (26);

B. multilateration
   - B.i) all neighbors of N_X;
   - B.ii) all robust neighbors of N_X by the criterion in [15];
   - B.iii) all robust neighbors of N_X by criterion (26).

An efficient flip ambiguity removal by the robustness criterion (26) in trilateration-based sequential localization is shown in Fig. 16. A numerical study in [18] shows that the location estimation errors are generally low, and a large variance in location estimation error occurs only due to flipped realization and the following avalanche effects. The ten-time-lower average estimation error of A.ii) and A.iii), and B.ii) and B.iii) compared with A.i) and B.i), respectively, in Fig. 17(a) and (c), can be interpreted as efficient flip ambiguity removal by the robustness criteria in the entire trilateration-based and multilateration-based sensor network localization.

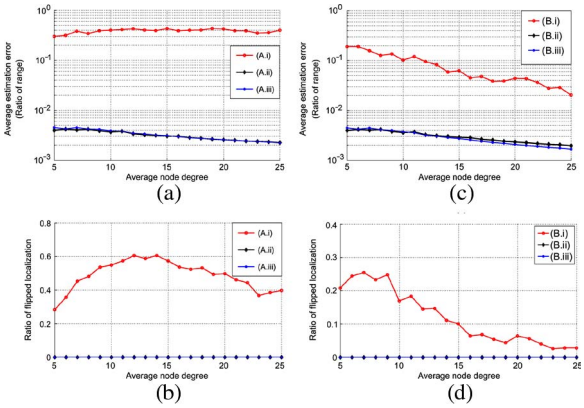

Fig. 17. Performance of different neighbor selection methods. (a) and (b) Trilateration-based sequential localization. (c) and (d) Multilateration-based sequential localization. Note that the curves (A.ii) and (A.iii) and (B.ii) and (B.iii) overlap each other and are hence not clearly conspicuous.

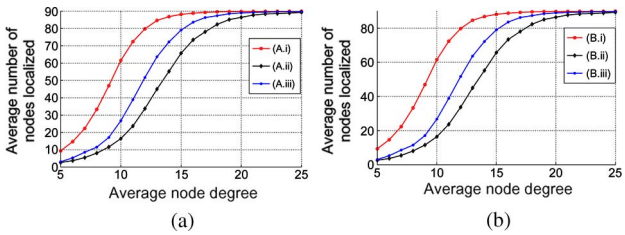

Fig. 18. Average localized nodes. (a) Trilateration-based sequential localization. (b) Multilateration-based sequential localization.

As discussed in Section VII, to simplify the flip detection, any estimation error $> R/5$ is treated as having substantial flip ambiguity. Fig. 17(b) and (d) shows the sensor network realization with possible flip ambiguities detected under this definition, and it can bee seen that neighbor selection methods A.i) and B.i) resulted in more flipped realizations in many sensor network realizations. This is an expected result, since the numerical study presented in Section VII showed that the robustness criterion removes all flip ambiguities when $\bar{\epsilon} \geq 3\sigma$. The numerical study also showed that the considerable amount of false alarms caused by the robustness criterion does not allow some of the location estimates to happen. This is the reason for the lower average localized nodes seen in A.ii) and A.iii), and B.ii) and B.iii) compared with A.i) and B.i), respectively, in Fig. 18.

It is worth noting here that the number of localized nodes using both trilateration and multilateration are the same and that the difference is in the estimation errors created by them. When the FCQs with possible flip ambiguity are not identified and removed from the localization process, multilateration helps remove some but not all flip ambiguities, creating less estimation error compared with its counterpart, i.e., trilateration. However, when the FCQs with possible flip ambiguity are identified and removed from the localization process, the difference in the estimation errors between the two methods are marginal, which is much smaller than the previous case.

The relationship of false alarm and missed detection with respect to the threshold $\bar{\epsilon}$ is seen in Section VII. To see the effect of the varying threshold $\bar{\epsilon}$ in the sensor network localizations, a second set of simulations are done with variable threshold $\bar{\epsilon}$ in the robustness criterion (26), where $\bar{\epsilon}$ is varied between

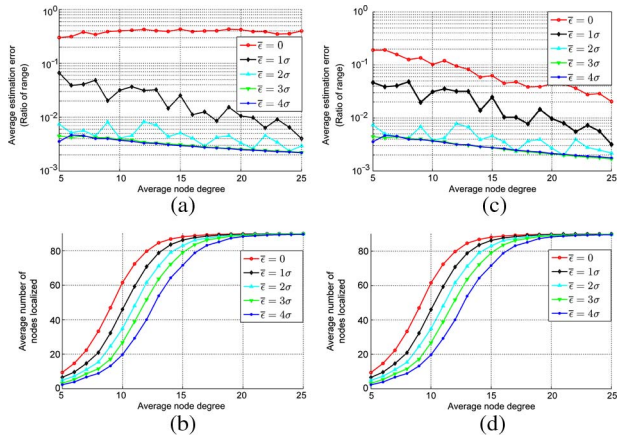

Fig. 19. Performance of different thresholds $\bar{\epsilon}$ in (26). (a) and (b) Trilateration-based sequential localization. (c) and (d) Multilateration-based sequential localization. Note that the curves $\bar{\epsilon} = 3\sigma$ and $\bar{\epsilon} = 4\sigma$ overlap each other in (a) and (c) and are hence not clearly conspicuous.

σ and 4σ. The results are shown in Fig. 19. As expected, the results show that the false alarm reduces with decreasing threshold $\bar{\epsilon}$, increasing the number of localized nodes. It also shows that missed detection increases with decreasing threshold $\bar{\epsilon}$, increasing the average estimation error of localized nodes.

IX. Threshold Effects and an Iterative Multithreshold Localization Method

A. Algorithm

As seen in Section VII, the robustness criterion with a larger threshold $\bar{\epsilon}$ may cause more false alarms. In such situations, more sensor nodes with three or more members in their neighbor set cannot be localized by the localization algorithm using our criterion. On the other hand, a smaller threshold $\bar{\epsilon}$ may cause more missed flip detection. In such situations, there may be more sensor nodes with faulty localization results. To prevent both of these situations, an iterative localization algorithm is presented in this section that can be applied to any of the localization algorithms presented in the last section.

This iterative localization method starts with a large threshold $\bar{\epsilon}_1$ to obtain an initial location estimate. In the subsequent iterations, the threshold $\bar{\epsilon}_{i-1}$ (for $i = 2, 3, \ldots$) is gradually reduced by a predefined step size $\Delta\bar{\epsilon}$ as $\bar{\epsilon}_i = \bar{\epsilon}_{i-1} - \Delta\bar{\epsilon}$ before using it in the robustness criterion. This reduction of $\bar{\epsilon}_i$ in each iteration causes a reduction in the number of false alarms and, in return, increases the number of localized nodes. This algorithm can be iterated until the threshold $\bar{\epsilon}_i$ reaches zero or some predefined minimum value $\bar{\epsilon}_{\min}$, which can be determined based on the required accuracy level of the location estimates.

After each iteration of the localization algorithm, the status of the sensor nodes localized in that iteration will be promoted to elevated anchor nodes. The subsequent iterations will not reestimate the locations of these elevated anchor nodes. Only the unknown sensor nodes with a robust neighbor set RN_X satisfying the robustness criterion with the reduced threshold $\bar{\epsilon}_i$ will be localized in the corresponding iteration step i. The reduction of threshold $\bar{\epsilon}_i$ at each subsequent iteration is likely to cause more missed detection, in return causing more flip ambiguities than in the previous iterations. Thus, the estimation

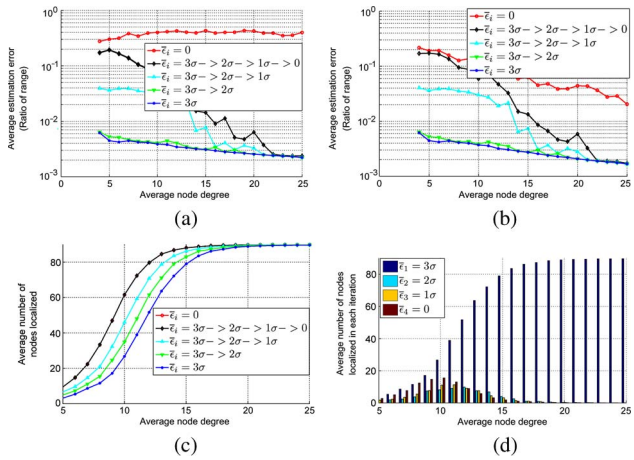

Fig. 20. Performance of the iterative process of the sequential localization. (a), (c), and (d) Trilateration-based sequential localization. (b), (c), and (d) Multilateration-based sequential localization. Note that the curves $\overline{\epsilon} = 0$ and $\overline{\epsilon}_i = 3\sigma - > 2\sigma - > 1\sigma - > 0$ are an exact match of each other in (c) and are hence inconspicuous.

error is likely to increase more in each subsequent iteration than in the previous iterations.

The iterative algorithm is summarized as follows, where the number of iterations n, $\overline{\epsilon}_n = \overline{\epsilon}_{\min}$, and $\overline{\epsilon}_1 = \overline{\epsilon}$ are predefined; the vertex set V_a represents the set of anchor nodes, and the vertex set V represents the complete set of sensors of the underlying network graph.

Algorithm 1 Iterative Multithreshold Localization Algorithm

1: $\overline{\epsilon}_1 \leftarrow \overline{\epsilon}$
2: $\Delta\overline{\epsilon} \leftarrow (\overline{\epsilon} - \overline{\epsilon}_{\min}/n)$
3: $V_0 \leftarrow V_a$
4: **for** $i = 1$ to n **do**
5: Apply localization algorithm with robustness criterion and threshold $\overline{\epsilon}_i$, to obtain the location estimates of the localizable sensors in $V \setminus \cup_{j=0}^{i-1} V_j$.
6: Label the set of newly localized sensors as V_i.
7: $\overline{\epsilon}_{i+1} = \overline{\epsilon}_i - \Delta\overline{\epsilon}$
8: **end for**

Using the iterative method described earlier, we obtain better localization accuracy of the sensor nodes than the localization accuracy that we would have obtained using a single threshold value.

B. Simulation Results

The performance of the iterative sequential localization algorithm is presented in this section. Even though the iterative cluster localization algorithm produces a similar result, due to page limitations, the corresponding simulation results are not presented in this paper. The simulations are done in four iterative steps by starting with a threshold value $\overline{\sigma} = 3\sigma$ and reducing it with a step size of $\Delta\epsilon = \sigma$ until the threshold $\overline{\epsilon}$ reaches zero. Each iteration of the sequential localization algorithm used the reduced threshold $\overline{\epsilon}$ in the robustness criterion (26), while taking all localized nodes of previous iterations as elevated anchors. The results of each iterative step are shown in Fig. 20. As noted in Section VIII-A2, both trilateration- and multilateration-based iterative localization algorithms localized the same number of sensor nodes. Hence, only the results of the multilateration-based iterative localization algorithm are presented in Fig. 20(c) and (d).

It can be seen from the results shown in Fig. 20 that our iterative localization algorithm significantly improves the number of localized sensor nodes (within an acceptable estimation errors) compared with the number of localized sensor nodes presented in Fig. 18.

X. Conclusion

In this paper, we have analyzed flip ambiguity problems and their implications in planar sensor network localization by a formal geometric analysis. We have quantified the likelihood of flip ambiguities in arbitrary sensor neighborhood geometries. We also have developed a robustness criterion that can identify the likelihood of flip ambiguity in FCQs, which are quadruples of sensor nodes, all of which are neighbors of each other, via a formal optimality analysis. This robustness criterion is used in localization algorithms to eliminate sensor nodes from any neighborhood that contribute to flip ambiguities. The simulation results demonstrate that the benefits of using our proposed robustness criterion are significant, and the criterion performs well in identifying flip ambiguities while causing a very small number of false alarms. The simulation results also show that the use of the robustness criterion in an iterative multithreshold localization method improves the number of localized nodes in a sensor network while keeping the accuracy of estimation errors at acceptable levels.

References

[1] S. Guolin, C. Jie, G. Wei, and K. Liu, "Signal processing techniques in network-aided positioning: A survey of state-of-the-art positioning designs," *IEEE Signal Process. Mag.*, vol. 22, no. 4, pp. 12–23, Jul. 2005.

[2] F. Gustafsson and F. Gunnarsson, "Mobile positioning using wireless networks: Possibilities and fundamental limitations based on available wireless network measurements," *IEEE Signal Process. Mag.*, vol. 22, no. 4, pp. 41–53, Jul. 2005.

[3] A. Sayed, A. Tarighat, and N. Khajehnouri, "Network-based wireless location: Challenges faced in developing techniques for accurate wireless location information," *IEEE Signal Process. Mag.*, vol. 22, no. 4, pp. 24–40, Jul. 2005.

[4] G. Mao, B. Fidan, and B. Anderson, "Wireless sensor network localization techniques," *Comput. Netw.*, vol. 51, no. 10, pp. 2529–2553, Jul. 2007.

[5] G. Mao, B. Fidan, and B. Anderson, "Sensor network localization," in *Sensor Network and Configuration: Fundamentals, Techniques, Platforms and Experiments*, N. P. Mahalik, Ed. New York: Springer-Verlag, 2006, pp. 281–316.

[6] Y. Shang, W. Ruml, Y. Zhang, and M. Fromherz, "Localization from connectivity in sensor networks," *IEEE Trans. Parallel Distrib. Syst.*, vol. 15, no. 11, pp. 961–974, Nov. 2004.

[7] P. Biswas and Y. Ye, "Semidefinite programming for ad hoc wireless sensor network localization," in *Proc. Inf. Process. Sens. Netw.*, 2004, pp. 46–54.

[8] A. Kannan, G. Mao, and B. Vucetic, "Simulated annealing based wireless sensor network localization with flip ambiguity mitigation," in *Proc. IEEE Veh. Technol. Conf.*, 2006, vol. 2, pp. 1022–1026.

[9] K. Langendoen and N. Reijers, "Distributed localization in wireless sensor networks: A quantitative comparison," *Comput. Netw.*, vol. 43, no. 4, pp. 499–518, Nov. 2003.

[10] V. Fox, J. Hightower, L. Lin, D. Schulz, and G. Borriello, "Bayesian filtering for location estimation," *IEEE Pervasive Comput.*, vol. 2, no. 3, pp. 24–33, Jul.–Sep. 2003.

[11] A. Ihler, I. Fisher, R. Moses, and A. Willsky, "Nonparametric belief propagation for self-localization of sensor networks," *IEEE J. Sel. Areas Commun.*, vol. 23, no. 4, pp. 809–819, Apr. 2005.

[12] J. Aspnes, T. Eren, D. Goldenberg, A. Morse, W. Whiteley, Y. Yang, B. Anderson, and P. Belhumeur, "A theory of network localization," *IEEE Trans. Mobile Comput.*, vol. 5, no. 12, pp. 1663–1678, Dec. 2006.
[13] R. Connelly, "Generic global rigidity," *Discrete Comput. Geometry*, vol. 33, no. 4, pp. 549–563, Apr. 2005.
[14] T. Eren, D. Goldenberg, W. Whiteley, Y. Yang, A. Morse, B. Anderson, and P. Belhuneur, "Rigidity, computation, and randomization in network localization," in *Proc. IEEE INFOCOM*, 2004, vol. 4, pp. 2673–2684.
[15] D. Moore, J. Leonard, D. Rus, and S. Teller, "Robust distributed network localization with noisy range measurements," in *Proc. 2nd ACM Conf. Embed. Netw. Sens. Syst.*, 2004, pp. 50–61.
[16] B. Hendrickson, "Conditions for unique graph realizations," *SIAM J. Comput.*, vol. 21, no. 1, pp. 65–84, Feb. 1992.
[17] D. Goldenberg, A. Krishnamurthy, W. Maness, Y. Yang, and A. Young, "Network localization in partially localizable networks," in *Proc. IEEE INFOCOM*, 2005, pp. 313–326.
[18] A. Kannan, B. Fidan, and G. Mao, "Robust distributed sensor network localization based on analysis of flip ambiguities," in *Proc. IEEE GLOBECOM*, 2008, pp. 1–6.
[19] S. Lederer, Y. Wang, and J. Gao, "Connectivity-based localization of large scale sensor networks with complex shape," in *Proc. IEEE INFOCOM*, 2008, pp. 789–797.
[20] Y. Wang, S. Lederer, and J. Gao, "Connectivity-based sensor network localization with incremental delaunay refinement method," in *Proc. IEEE INFOCOM*, 2009, pp. 2401–2409.
[21] Z. Yang, Y. Liu, and X. Li, "Beyond trilateration: On the localizability of wireless ad-hoc networks," in *Proc. IEEE INFOCOM*, 2009, pp. 2392–2400.
[22] D. Niculescu and B. Nath, "Dv based positioning in ad hoc networks," *Telecommun. Syst.*, vol. 22, no. 1–4, pp. 267–280, Jan. 2003.
[23] A. Savvides, C. C. Han, and M. B. Srivastava, "Dynamic fine-grained localization in ad-hoc networks of sensors," in *Proc. ACM SigMobile*, 2001, pp. 166–179.
[24] S. Capkun, M. Hamdi, and J. Hubaux, "Gps-free positioning in mobile ad-hoc networks," in *Proc. 34th Hawaii Int. Conf. Syst. Sci.*, 2001, pp. 3481–3490.
[25] F. Sittile and M. Spirito, "Robust localization for wireless sensor networks," in *Proc. IEEE SECON*, 2008, pp. 46–54.
[26] A. Kannan, B. Fidan, G. Mao, and B. Anderson, "Analysis of flip ambiguities in distributed network localization," in *Proc. Inf., Decision Control*, 2007, pp. 193–198.
[27] J. Fang, M. Cao, A. Morse, and B. Anderson, "Localization of sensor networks using sweeps," in *Proc. IEEE Conf. Decision Control*, 2006, pp. 4645–4650.
[28] D. Goldenberg, P. Bihler, M. Cao, J. Fang, B. Anderson, A. Morse, and Y. Yang, "Localization in sparse networks using sweeps," in *Proc. ACM/IEEE MobiCom*, 2006, pp. 110–121.
[29] B. Anderson, P. Belhumeur, T. Eren, D. Goldenberg, A. Morse, W. Whiteley, and R. Yang, "Graphical properties of easily localizable sensor networks," *Wireless Netw.*, vol. 15, no. 2, pp. 177–191, Feb. 2009.
[30] C. Savarese and J. Rabaey, "Robust positioning algorithms for distributed ad-hoc wireless sensor networks," in *Proc. General Track: USENIX Annu. Techn. Conf.*, 2002, pp. 317–327.
[31] C. Savarese, J. Rabaey, and J. Beutel, "Location in distributed ad-hoc wireless sensor networks," in *Proc. ICASSP*, 2001, pp. 2037–2040.
[32] L. Meertens and S. Fitzpatrick, "The distributed construction of a global coordinate system in a network of static computational nodes rom inter-node distances," Kestrel Institute, Palo Alto, CA, Formal Rep. KES.U.04.04, 2004.
[33] X. Ji and H. Zha, "Sensor positioning in wireless ad-hoc sensor networks using multidimensional scaling," in *Proc. IEEE INFOCOM*, 2004, vol. 4, pp. 2652–2661.
[34] Y. Shang and W. Ruml, "Improved MDS-based localization," in *Proc. IEEE INFOCOM*, 2004, vol. 4, pp. 2640–2651.
[35] Y. Kwon, K. Mechitov, S. Sundresh, W. Kim, and G. Agha, "Resilient localization for sensor networks in outdoor environments," in *Proc. IEEE ICDCS*, 2005, pp. 643–652.
[36] N. Patwari, A. Hero, III, M. Perkins, S. Neiyer, and R. ODea, "Relative location estimation in wireless sensor networks," *IEEE Trans. Signal Process.*, vol. 51, no. 8, pp. 2137–2148, Aug. 2003.

Anushiya A. Kannan (M'08) received the B.Sc. and B.E. degrees, in 1994 and in 1995, respectively, from the University of Sydney, Sydney, Australia, where she is currently working toward the Ph.D. degree in wireless sensor networks.

She has been with TriTech Microelectronics, Singapore; Adaptive Broadband, Cambridge, U.K.; and Cellonics, Singapore. She is currently a Researcher with the Biomedical Systems Laboratory, University of New South Wales, Sydney. Her research interests include wireless sensor networks, wireless communications, biomedical engineering, and integrated circuit design.

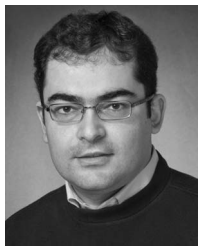

Barış Fidan (M'03) received the B.S. degrees in electrical engineering and mathematics from Middle East Technical University, Ankara, Turkey, in 1996, the M.S. degree in electrical engineering from Bilkent University, Ankara, in 1998, and the Ph.D. degree in electrical engineering from the University of Southern California, Los Angeles, in 2003.

He was with the University of Southern California in 2004 as a Postdoctoral Research Fellow and with the National ICT Australia and the Research School of Information Sciences and Engineering, Australian National University, during 2005–2009 as a Researcher/Senior Researcher. He is currently an Assistant Professor with the Department of Mechanical and Mechatronics Engineering, University of Waterloo, Waterloo, ON, Canada. His research interests include autonomous multiagent dynamical systems, sensor networks, cooperative localization, adaptive and nonlinear control, switching and hybrid systems, mechatronics, and various control applications, including high-performance and hypersonic flight control, semiconductor manufacturing process control, and disk-drive servo systems.

Guoqiang Mao (SM'08) received the Bachelor's degree in electrical engineering from Hubei Polytechnic University, China, in 1995, the Master's degree in engineering from South East University, Nanjing, China, in 1998, and the Ph.D. degree in telecommunications engineering from Edith Cowan University, Perth, Australia, in 2002.

In December 2002, he joined the School of Electrical and Information Engineering, University of Sydney, Sydney, Australia, where he is currently a Senior Lecturer. He has published more than 70 papers in journals and refereed conference proceedings. His research interests include wireless localization techniques, wireless multihop networks, graph theory and its application in networking, and network performance analysis.

Dr. Mao has served as a program committee member at a number of international conferences and was the publicity co-chair of the 2007 ACM SenSys and the publicity co-chair of the 2010 IEEE Wireless Communications and Networking Conference.